JOURNAL OF OPTOELECTRONICS AND ADVANCED MATERIALS Vol. 12, No. 4, April 2010, p. 858 - 863

Probing magnetic fluid nanoparticle aggregation in aqueous suspensions by coherent light scattering anisotropy measurement

D. CHICEA
Physics Dept., University Lucian Blaga of Sibiu, Dr. Ion Ratiu Str. 7-9, Sibiu, 550012, Romania

Light scattering on particles having the diameter comparable with the wavelength is accurately described by the Mie theory and the light scattering anisotropy can conveniently be described by the one parameter Henyey Greenstein phase function. An aqueous suspension containing magnetite nanoparticles was the target of a coherent light scattering experiment. By fitting the scattering phase function on the experimental data the scattering anisotropy parameter can be assessed. As the scattering parameter strongly depends of the scatterer size, the average particle diameter was thus estimated and particle aggregates presence was probed. This technique was used to investigate the nanoparticle aggregation dynamics and the results are presented in this work.

(Received April 7, 2010; accepted April 26, 2010)

Keywords: Light scattering anisotropy, Suspensions, Nanofluids, Aggregates

1. Introduction

When a small amount of nanoparticles is added to a fluid, the heat transfer properties are considerably enhanced [1]. Such a suspension is currently named a nanofluid; it is a relatively new notion and was first mentioned by Choi in 1995 [2].

The nanoparticles have a continuous, irregular motion in nanofluids, which is the effect of several factors such as gravity, Brownian force, Archimede's force and friction force between fluid and the particles. The irregular nanoparticle motion in the fluid is the cause the remarkable enhancement of heat transfer properties of the nanofluids [3-6]. The irregular motion directly depends of the particle dimension therefore the particle size distribution dictates the rheological properties of the nanofluid.

Nanoparticles in aqueous suspensions naturally aggregate forming clusters of colloids with an isotropic shape, most probably caused by van der Waals attractions and weak magnetic attractions, which are both of the order of kT [7]. Cobalt nanoparticle are reported to aggregate in "bracelets" [8] which are distinct from the micrometer-sized rings created by rapidly evaporating films of dispersed nanoparticles, with regard to ring size (typically 5-12 particles and 50-100 nm in diameter). [9] Describes the preparation of robust micrometer size ring structures on mica surfaces. Ring shaped clusters of Co-PFS were patterned onto a thin gold film sputtered onto a silicon wafer that had been primed with a 5 nm layer of titanium as is reported in [10]. The clusters mentioned in [10] have diameters between 0.6 and 12 μm.

Particle aggregation has been extensively studied on different systems containing micron and nanometer size particles in suspension. Transmission Electron Microscopy (TEM) is currently used in characterizing nanoparticles and nanometer to micrometer sized clusters. While it offers the best resolution, the sample requires specific preparation to be shaped as a very thin film and finally is placed in vacuum and becomes target for the electron beam, thus TEM can not be used for in situ investigations.

The work presented here was carried on to investigate the dynamics of nanoparticle aggregates formation in diluted aqueous suspension, therefore a light scattering technique was employed.

A typical approach uses a coherent light scattering experiment. The target is the suspension, the far field is recorded and the statistical analysis of the speckle image is performed. The speckled image appears as a result of the interference of the wavelets scattered by the scattering centers (SC hereafter), each wavelet having a different phase and amplitude in each location of the interference field. The image changes in time as a consequence of the scattering centers complex movement of sedimentation and Brownian motion giving the aspect of "boiling speckles" [11], [12]. In papers like [13] an optical set-up is used to measure the correlation function in the near field, and reveals the near-field speckle dependence on the particles size. The work reported in [14], [15] uses a transmission optical set-up to measure the far field parameters like contrast and speckle size and reveals that speckle size and contrast are related with the average particle diameter. Reference [16] revealed a strong variation of the average speckle size and contrast with the concentration of the scattering centers. In a diluted aqueous suspension as aggregates are formed, both the concentration and the size of the scattering centers change in time, therefore these far field parameters, speckle size and contrast are not suited for monitoring the nanoparticle aggregation process.

Another system that contains scattering centers and presents a particular interest in medicine is the human blood. Coherent light propagation through biological cells in suspensions or tissues has been studied for quite a long time. Platelets are highly sensitive blood cells with an important physiological role in hemostasis. Platelets can be activated or inhibited under small influences and consequently their response to the basic physiological agonists must be characterized by easy to handle tools, therefore particle aggregation techniques have been developed. For several decades the basic method of studying platelets aggregation has been the Born technique based on the increase in light transmission [17]. In the last several years light scattering techniques entered the attention of scientific community as alternative methods. The first idea was to use the information offered by the backward scattered light [18], technique that works well in the single scattering regime recording the light scattered backward by separate particles or their aggregates. The method was used afterward for measurements on platelet rich plasma. Other development reported in the literature was applied to aggregation studies [19].

More recent, the time dependent forwardly scattered light was detected by a photodiode array in the angular range 1 - 15 degrees and used to describe the kinetics of platelet aggregation [20], [21]. Two angular domains with qualitatively different behaviors were clearly evidenced by the reported measurements. Below 6 degrees, the signal given by the photodiodes increase as the platelets turn into aggregates while the signal for higher angles 6 - 15 degrees decreases. The effect is explained by de dependence of the light scattering anisotropy by the size of the scattering object.

Another interesting procedure for monitoring the particle aggregation in human rich platelet plasma was resented in [22] and consists of monitoring the scattered light intensity variation at a certain small angle in 1.5 – 4 degrees range. A quantitative procedure in terms of two parameters first order Hill function to describe the platelets aggregation kinetics is presented as well, in [22].

In this work the Henyey-Greenstein phase function is used to describe light scattering on suspensions. The variation of the scattering anisotropy parameter with the diameter of the scattering center (SC hereafter), as results from Mie calculation, is used to describe in a half quantitative way the aggregation process in diluted magnetic fluid. Details on the theoretical phase function and on the experimental setup and results are presented in the next sections.

2. Light scattering anisotropy

Several empirical phase functions are frequently used to describe light scattering on biological suspensions; among them the Henyey–Greenstein phase function (1) and the two parameters Gegenbauer kernel phase function are the most commonly used [23], [24], [25].

$$f(\mu)=\frac{1}{2}\frac{1-g^2}{\left(1-2\mu g+g^2\right)^{\frac{3}{2}}} \tag{1}$$

In (1) $\mu = \cos(\theta)$, θ is the polar scattering angle and $g=\langle\mu\rangle$ is the scattering anisotropy parameter.

The Henyey Greenstein phase function can not be measured directly. A detector has a finite transversal dimension d and can be seen from the active part of the cuvette as covering a certain solid angle, hence a polar angle interval [θ1, θ2]. The light intensity that can be measured using a detector is proportional with the integral of the phase function over the polar angle interval [θ1, θ2], which is:

$$F(\mu_1,\mu_2)=\int_{\mu_1}^{\mu_2} f(\mu)d\mu=\frac{\left(1-g^2\right)}{g}\left[\frac{1}{\sqrt{1+g^2-2g\mu_1}}-\frac{1}{\sqrt{1+g^2-2g\mu_2}}\right] \tag{2}$$

where:

$$\mu_1=\cos\theta_1,\quad \mu_2=\cos\theta_2 \tag{3}$$

Equation (2) was used in the experimental work reported here to verify the effective phase function described above.

Moreover, the intensity that can be recorded using a detector is the result of the interference of the wavelets scattered by the scattering centers (SC hereafter), each wavelet having a different phase and amplitude in each location of the interference field. Thus an un-uniformly illuminated image is obtained, currently named speckled image, having a statistical distribution of the intensity over the interference field. The speckled image can be observed either in free space and is named objective speckle or on the image plane of a diffuse object illuminated by a coherent source; it is named subjective speckle in [23]. The review paper [24] classifies the two types of speckled images as far field speckle and image speckle. In this work the objective speckle, respectively far field speckle is considered. The image changes in time as a consequence of the scattering centers complex movement of sedimentation and Brownian motion giving the aspect of "boiling speckles" [23], [24]. Consequently the signal recorded over a time interval must be averaged in order to compensate the "boiling speckles" fluctuations.

Coming back to the Henyey–Greenstein phase function (1), we can model light scattering on nanoparticle and nanoparticle clusters as light scattering on spherical particles having diameters in the range 0.05 – 15 μm and the refractive index equal to 1.45, which is a typical value for glassy substances. The spheres are considered to be in suspension in water, having the refractive index equal to 1.333.

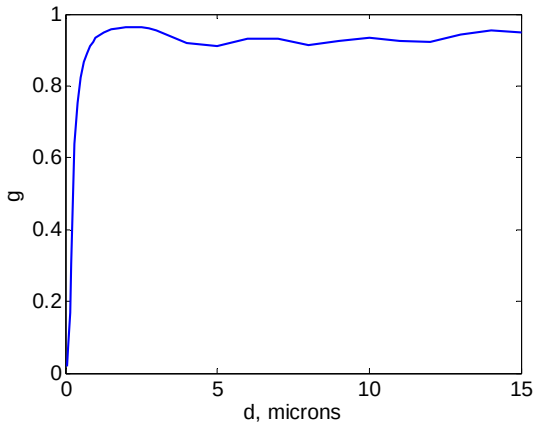

Fig. 1. The variation of the scattering anisotropy parameter g for magnetite spherical particles in aqueous suspension with the nanoparticle diameter.

Fig. 1 presents the results of g Mie calculations [26], [27] in the frame of the simple model described above, for different diameters in the range 0.05 – 15 μm. Examining Fig. 1 we notice a very fast increase of the g value in the very small diameter range and a plateau with small variations for spheres having the diameter in the microns range. The variation of the g parameter with the diameter can be used to assess the average particle diameter in suspension. The next sections describes the experimental procedure and the results.

3. Experimental setup, data processing

The nanofluid was a suspension of Fe_3O_4 nanoparticles having citric acid as surfactant. Details on nanofluid preparation are presented in [28].

The experimental setup consists of a He-Ne laser having the wavelength of 632 nm and a constant power of 2 mW, a cuvette, a sensitive detector, a CCD and a computer. First the detection system was calibrated. The calibration procedure provides the functional dependence of the grey level recorded by a certain cell on the CCD matrix in a bitmap or on a frame of an AVI type movie with the light intensity. A schematic of the experimental setup is presented in Fig. 2.

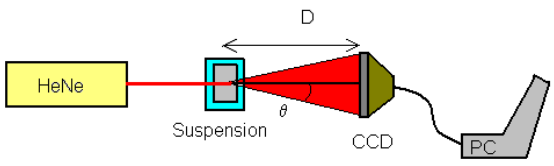

Fig. 2. The schematic of the experimental setup, view from above.

The main hint of the experimental setup, as presented in [22] is to record the far interference field directly on the CCD and to capture a bitmap. Thus each individual cell becomes a detector and by extracting the light intensity recorded by a consecutive set of cells in an array a light intensity versus scattering angle profile can be extracted. In order to do that D and the size of a cell on the CCD must be precisely measured. D was adjusted during the experiment to cover the desired angular interval, 0.45 – 2.10 °, in the 10-30 cm range. The cell on the CCD is square and the side of the cell is 5.83 μm.

A bitmap of the far field scattered light on diluted nanofluid suspension is presented in Fig. 3. Examining it we notice the speckle aspect. The resolution of each bitmap was 480 x 640 and the averages were performed on 10 seconds of recording. A horizontal profile extracted from the bitmap area where the direct beam hits the CCD presented in Fig. 3 is presented in Fig. 4.

Examining Fig. 4 we notice a decrease of the intensity outside the saturated area where the direct beam hits the CCD, but the speckle effect, described in the previous section makes this type of profile improper for fitting the integral of the Henyey – Greenstein in (2) on it and expecting accurate results in respect of the g parameter.

In order to compensate the fluctuations that give the speckle aspect a movie was recorded for each sample subject to particle aggregation study. The framerate must be adjusted accordingly to the size of the SCs. The bigger is the diameter the slower is the fluctuation rate.

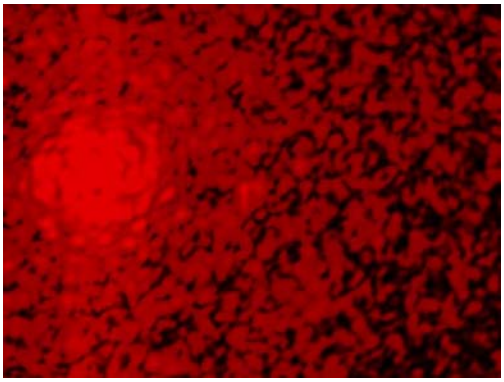

Fig. 3. A bitmap of the far field scattered light on diluted nanofluid.

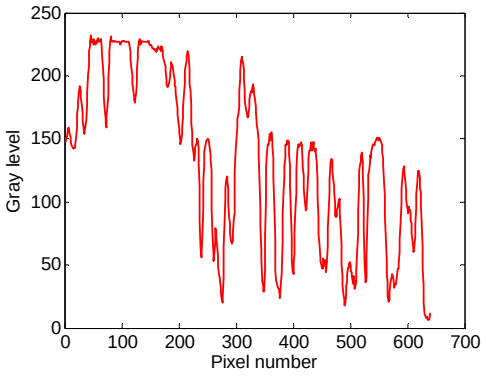

Fig. 4. A horizontal intensity profile extracted from the bitmap in Fig. 3, corresponding to the 240-th row.

The movie is processed later on using a computer program written for this purpose [16]. The program reads sequences of successive frames. The number of frames in a sequence is calculated accordingly with the input parameter that indicates the time step for calculating the average scattering parameter g, 10 seconds for the work presented here. From each frame the intensity levels recorded by an array of cells being as wide (high) as the spot, 170 pixels for the experiments reported here, and as long (wide) as the width of the CCD minus the saturated area, 440 for the experiments reported here, is extracted. Averages are performed on each individual sequence of frames and on each vertical set of 170 pixels, the light intensity is finally calculated using the calibration curve and an averaged intensity profile versus angle is produces for each sequence, hence moment from the beginning of the recording. The abscissa is expressed in angles. An averaged profile is presented in the next section in Figs. 5 and 6 revealing that the speckle fluctuations were considerably reduced.

As the program reads the whole movie and processes it, an averaged profile is produces for each sequence and allotted to the middle of the time interval it was extracted from.

Another program written for this purpose reads each scattering profile in batch mode and fits the integrated Henyey – Greenstein in (2) multiplied by a constant C proportional to the laser beam intensity on it. The fit outputs the values of C and g that produces the best fit for each profile. The variation of the scattering parameter g with the time elapsed from the beginning of the experiment can be plotted and analyzed. Experimental results using the procedure presented in this section are presented in the next section.

4. Experimental results

The first analyzed type of suspension that was was a suspension of magnetite nanoparticles having citric acid as surfactant. The magnetite nanoparticles were produced using reaction (4) and details are presented in [28].

$$2\,FeCl_3 + FeCl_2 + 8NH_3 + 4H_2O \rightarrow Fe_3O_4 + 8NH_4Cl \quad (4)$$

The concentration was 1.6% volume ratio nanoparticles in deionized water at 20°C. Dilution was made in a beaker and the sample was poured in a 10 mm thick cuvette. The whole procedure of dilution and pouring the nanofluid in the cuvette was practiced several times to make it as fast as possible and finally lasted less than one minute. In this way the recording started after precisely one minute since the beginning of the dilution process; t=0 on the plot in Fig. 7 means one minute after the fast dilution process started.

Fig. 5 presents the average intensity profile for the first 10 seconds, allotted to t=5 s, and the result of the fit using (2), the smooth line, as described in the previous section. We notice that the profile is smoother than in Fig. 4 and that the scattering parameter is 0.98207, corresponding to spherical particles with the diameter around 2 microns.

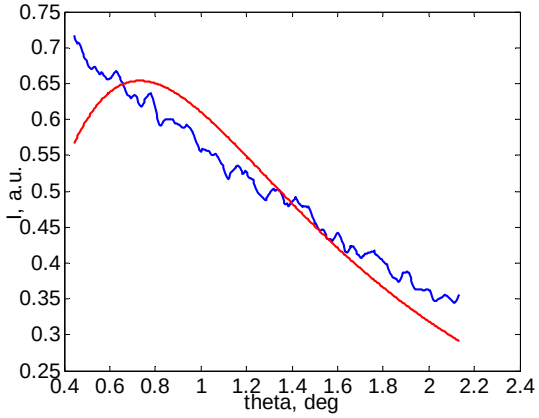

Fig. 5. The intensity profile for the first 10 seconds and the result of the Henyey Greenstein phase function fit, using (2), the smooth line.

Fig. 6 presents the average intensity profile for the 42-nd sequence of 10 seconds, allotted to t=415 s, and the result of the fit using (2). We notice that the profile has smaller values than the profile averaged on the first 10 seconds and that the scattering parameter is 0.98161, corresponding to spherical particles with a diameter around 5 microns or bigger, according to Fig. 1.

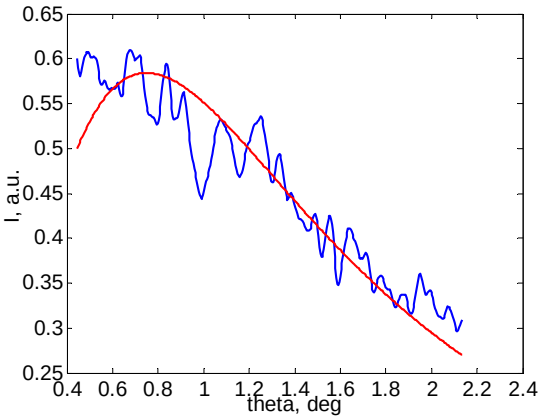

Fig. 6. The intensity profile for the time interval centered on 415 s and the result of the Henyey Greenstein phase function fit, using (2), the smooth line.

The variation of the scattering parameter with the time elapsed from the beginning of the experiment, calculated using the procedure described in the previous section, is presented in Fig. 7. The experiment was repeated four times and there is no significant difference in the results.

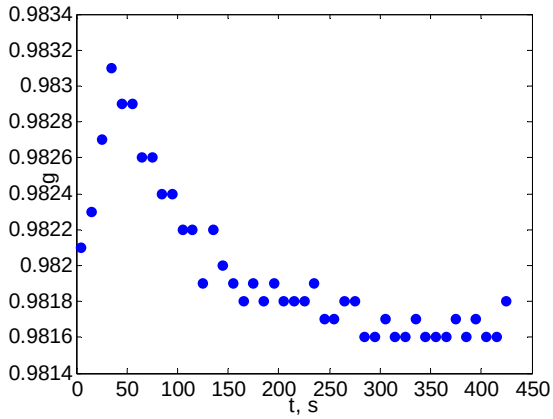

Fig. 7. The variation of the scattering parameter with the time.

Examining Fig. 7 we notice a fast increase of the light scattering parameter g in time after nanoparticle dillution started. The fast increase can be explained by aggregates formation in the diluted nanofluid. The increase actually lasts for two minutes since dilution started. As the recording started one minute after the fast dilution was initiated, we notice that big clusters were already present at that time in a sufficient number to considerably change the scattering parameter from small values, around 0.17, which corresponds to 150 nm diameter particles.

Fig. 7 reveals that as time passes the scattering parameter decreases slowly and finally displays a plateau. This is consistent with the presence of larger sized aggregates in bigger number. The scattering parameter values on the plateau in Fig. 7 correspond to the part of the plot in Fig 1 with diameters bigger than 4 microns.

In order to understand the variation of the scattering parameter in time, we should keep in mind that for small particles, comparable with the wavelength, Rayleigh approximation can be used to describe light scattering [29]. As the particle diameter *d* increases, at constant volume ratio, the nanoparticles number *N* should vary with the diameter *d* as:

$$N = \frac{V_{nano}}{\frac{4\pi}{3}\cdot\left(\frac{d}{2}\right)^3} \tag{4}$$

where V_{nano} is the total nanoparticle volume in suspension. Light scattering on nanoparticles is a Rayleigh type scattering, therefore the light intensity scattered by one individual particle is proportional to d^6 [29]. The average intensity scattered by all the nanoparticles in the sample and recorded at a constant angle is therefore proportional to d^3, thus increasing with the nanoparticle cluster diameter, as revealed by eq, (5).

$$< I > \approx N \cdot < I(\theta) > \approx \left(\frac{d}{2}\right)^3 \tag{5}$$

We notice from (5) that the light intensity scattered by one cluster having a diameter in the range of microns is roughly 10^9 larger that the intensity scattered by one nanoparticle, therefore the far field landscape becomes dominated by light scattered by clusters, as soon as they appear. The light scattering parameter g calculated using the procedure described in the previous section is actually the parameter of light scattered by clusters.

Consequently the procedure described above is not sensitive in respect of measuring the amount of nanoparticles that turned into aggregates, but to reveal the presence of aggregates.

Nevertheless, the experiment reveals that the procedure can be used for a half quantitative assessment of the time elapsed from the beginning of the dilution to the moment when cluster formation is completed in an aqueous suspension. During the first minute a significant amount of nanoparticles turned into aggregates and the aggregate dimension is growing. After two minutes the aggregates reached the value of the maximum scattering parameter, which, for magnetite is around 2 microns. The further size increase can not be monitored using this procedure, because the scattering parameter presents very small variations as the diameter increases further on, accordingly to Fig. 1. After 6 minutes since the dilution started, the scattering parameter remains constant, in the limits of the experimental errors and of the systematic errors, therefore we can conclude that an equilibrium has been reached in aggregates formation.

5. Conclusions

In this work a simple experimental procedure, assisted by a set of computer programs required to process data is presented. The procedure consists of recording, using a CCD, an AVI type of movie containing light scattered at small angles by suspensions. The average light scattering intensity versus scattering angle is recorded and the light scattering parameter g is calculated using a least squares fit. The time variation of the g parameter is compared with the Mie theoretical variation of the g parameter with the particle diameter.

By comparing the measured value of the g with the theoretical curve g versus diameter, at least in a half quantitative way, the procedure described in this paper might be an alternative to the procedures described in [13 - 22] for monitoring particle aggregation in suspension.

Using this procedure we found that magnetite nanoparticles having citric acid as surfactant, in aqueous diluted suspension, 1.6%, aggregate very fast. During the first two minutes the aggregates dimension increases and the size reaches 2 microns. It increases further on but the procedure described in this paper is not sensitive for bigger diameter aggregates. After six minutes from the beginning of the experiment equilibrium has been reached.

Further improvement can be done by preparing the diluted suspension in the cuvette and excluding the contribution of the turbulence to the scattering parameter g.

References

[1] P. Vadasz, J. Heat Transfer. **128**, 465 (2006).
[2] U. S. Choi, ASME Fed. **231**, 99 (1995).
[3] S. P. Jang and S. U. S. Choi, Appl. Phys. Lett. **84**, 4316 (2004).
[4] W. Evans, J. Fish and P. Keblinski, Appl. Phys. Lett. **88**, 093116 (2006).
[5] Y. M. Xuan and W. Roetzel, Int. J. Heat Mass Transfer. **43**, 3701 (2000).
[6] R. Prasher, P. Brattacharya, P. E. Phelan, Phys. Rev. Lett. **94**, 025901 (2005).
[7] K. Butter, P. H. Bomans, P. M. Frederik, G. J. Vroege, A. P. Philipse, J. Phys.: Condens. Matter **15**, S1451, (2003). doi: 10.1088/0953-8984/15/15/310.
[8] S. L. Tripp, S. V. Pusztay, A. E. Ribbe, A. Wei, J. Am. Chem. Soc. **124**, 7914 (2002).
[9] Z. Xiao, C Cai, X. Deng, Chem. Commun., 1442–1443, 2001. DOI: 10.1039/b104306b.
[10] S. B. Clendenning, S. F. Bidoz, A. Pietrangelo, G. Yang, S. Han, P. M. Brodersen, C. M. Yip, Z Lu, G. A. Ozin, I. Manners, J . Mater . Chem., **14**, 1686 (2004).
[11] J. W. Goodman, Laser speckle and related phenomena, Vol. 9 in series Topics in Applied Physics, J.C. Dainty, Ed., Springer-Verlag, Berlin, Heidelberg, New York, Tokyo, (1984).
[12] J. David Briers, Physiol. Meas. **22,** R35 (2001).
[13] M. Giglio, M. Carpineti, A. Vailati, D. Brogioli, Appl. Opt. **40**, 4036 (2001).
[14] Y. Piederrière, J. Cariou, Y. Guern, B. Le Jeune, G. Le Brun, J. Lotrian, Optics Express **12**, 176, (2004).
[15] Y. Piederriere, J. Le Meur, J. Cariou, J. F. Abgrall, M. T. Blouch, Optics Express **12**, 4596, (2004).
[16] D. Chicea, European Physical Journal Applied Physics **40**, 305 (2007), DOI: 10.1051/epjap:2007163
[17] G. V. R. Born, J. Physiol. **209**, 487 (1970).
[18] Y. Ozaki, K. Satoh, Y. Yatomi, T. Yamamoto, Y. Shirasawa, S. Kume, Anal. Biochem. **218**, 284 (1994).
[19] K. Yabusaki, E. Kokufuta, Langmuir. **18**, 39 (2002).
[20] I. V. Mindukshev, I. E. Jahatspanian, N. V. Goncharov, R. O. Jenkins, A. I. Krivchenk, Spectroscopy – Int. J. **19**, 235 (2005).
[21] I. V. Mindukshev, E. E. Ermolaeva, E. V. Vivulanets, E. Yu. Shabanova, N. N. Petrishchev, N. V. Goncharov, R. O. Jenkins, A. I. Krivchenko, Spectroscopy – Int. J. **19**, 247 (2005).
[22] Ioan Turcu, Silvia Neamtu, Cristian V. L. Pop, Int. Conf. on Isotopic Processes PIM5, 2007.
[23] M. Hammer, D. Schweitzer, B. Michel, E. Thamm, A. Kolb, Appl. Opt. **37**, 7410 (1998).
[24] M. Hammer, A. N. Yaroslavsky, D. Schweitzer, Phys. Med. Biol. **46**, N65 (2001).
[25] L. O. Reynolds, N. J. McCormick, J. Opt. Soc. Am **70**, 1206 (1980).
[26] S. Prahl's Mie online calculator at: http://omlc.ogi.edu/calc/mie_calc.html
[27] S. A. Prahl, M. Keijzer, S. L. Jacques, A. J. Welch, SPIE Proceedings of Dosimetry of Laser Radiation in Medicine and Biology, volume IS **5**, 102 (1989).
[28] D. Chicea, C. M. Goncea, Optoelectron. Adv. Mater. – Rapid Comm. **3**(3), 185 (2009).
[29] C. F. Bohren, D. Huffman, Absorption and scattering of light by small particles, John Wiley, New York (1983).

Corresponding author: dan.chicea@ulbsibiu.ro